

VLUC: An Empirical Benchmark for Video-Like Urban Computing on Citywide Crowd and Traffic Prediction

RENHE JIANG*, The University of Tokyo

ZEKUN CAI*, The University of Tokyo

ZHAONAN WANG, The University of Tokyo

CHUANG YANG, The University of Tokyo

ZIPEI FAN, The University of Tokyo

XUAN SONG, SUSTech-UTokyo Joint Research Center on Super Smart City, Department of Computer Science and Engineering, Southern University of Science and Technology (SUSTech)

KOTA TSUBOUCHI, Yahoo Japan Corporation

RYOSUKE SHIBASAKI, The University of Tokyo

Nowadays, massive urban human mobility data are being generated from mobile phones, car navigation systems, and traffic sensors. Predicting the density and flow of the crowd or traffic at a citywide level becomes possible by using the big data and cutting-edge AI technologies. It has been a very significant research topic with high social impact, which can be widely applied to emergency management, traffic regulation, and urban planning. In particular, by meshing a large urban area to a number of fine-grained mesh-grids, citywide crowd and traffic information in a continuous time period can be represented like a video, where each timestamp can be seen as one video frame. Based on this idea, a series of methods have been proposed to address video-like prediction for citywide crowd and traffic. In this study, we publish a new aggregated human mobility dataset generated from a real-world smartphone application and build a standard benchmark for such kind of video-like urban computing with this new dataset and the existing open datasets. We first comprehensively review the state-of-the-art works of literature and formulate the density and in-out flow prediction problem, then conduct a thorough performance assessment for those methods. With this benchmark, we hope researchers can easily follow up and quickly launch a new solution on this topic.

CCS Concepts: •**Information systems** → **Information systems applications**; **Geographic information systems**; •**Computing methodologies** → **Artificial intelligence**; •**Human-centered computing** → **Ubiquitous and mobile computing**;

Additional Key Words and Phrases: big data, human mobility, urban computing, deep learning

ACM Reference format:

Renhe Jiang*, Zekun Cai*, Zhaonan Wang, Chuang Yang, Zipei Fan, Xuan Song, Kota Tsubouchi, and Ryosuke Shibasaki. 2019. VLUC: An Empirical Benchmark for Video-Like Urban Computing on Citywide Crowd and Traffic Prediction. *PACM Interact. Mob. Wearable Ubiquitous Technol.* 0, 0, Article 0 (2019), 23 pages.
DOI: 12.1234/1234567

*Equal contribution.

Permission to make digital or hard copies of all or part of this work for personal or classroom use is granted without fee provided that copies are not made or distributed for profit or commercial advantage and that copies bear this notice and the full citation on the first page. Copyrights for components of this work owned by others than ACM must be honored. Abstracting with credit is permitted. To copy otherwise, or republish, to post on servers or to redistribute to lists, requires prior specific permission and/or a fee. Request permissions from permissions@acm.org.

© 2019 ACM. 2474-9567/2019/0-ART0 \$15.00

DOI: 12.1234/1234567

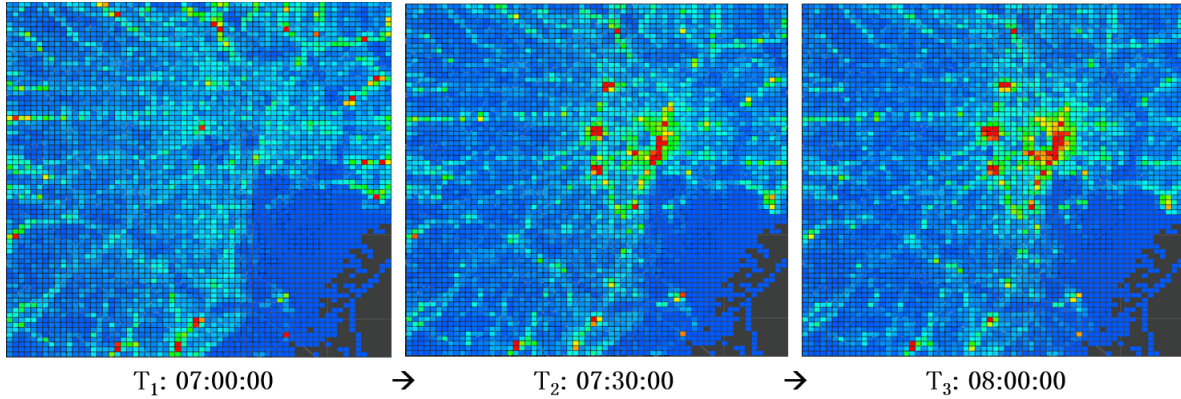


Fig. 1. An illustration of citywide crowd density in Tokyo from 07:00:00 to 08:00:00 is shown above, where the red color represents higher density and the blue color represents lower density. By meshing a large urban area to a number of fine-grained mesh-grids, citywide crowd density in a continuous time period can be analogously seen as a short video.

1 INTRODUCTION

Nowadays, massive urban human mobility data are being generated from mobile phones, car navigation systems, and traffic sensors. Many studies have analyzed these big mobility data with cutting-edge technologies, which have been summarized as urban computing by [60]. In particular, crowd or traffic prediction at a citywide level becomes an emerging topic in both academia and industry, as it can be of great importance for emergency management, traffic regulation, and urban planning. As illustrated in Fig.1, by meshing a large urban area to a number of fine-grained mesh-grids, citywide crowd and traffic information in a continuous time period can be represented with a four-dimensional tensor $\mathbb{R}^{Timestep \times Height \times Width \times Channel}$ in an analogous manner to video data, where each *Timestep* can be seen as one video frame, *Height*, *Width* is two-dimensional index for mesh-grids, and each *Channel* stores an aggregated scalar value for each mesh-grid. Following this representation, as shown in Table 1, a series of studies [13, 17, 24, 42, 47, 48, 53, 55–59, 62] have been conducted to address video-like urban computing problems such as crowd in-out flow prediction, taxi demand prediction, and traffic accident prediction. These forecasts can be provided to governments (e.g. police) and public service operators (e.g. subway or bus company) to protect people’s safety or maintain the operation of public infrastructures under event situation (e.g. New Year Countdown); to ride-sharing companies like Uber and Didi Chuxing to more effectively dispatch the taxis; to web mapping services like Yahoo Map¹ and Itsumo-Navi² to improve the functionality of crowd density map service.

“Urban video” containing citywide crowd and traffic information are high-dimensional sequential data with high complexity, which naturally drive researchers to design advanced deep learning models to achieve superior performance to classical methodologies. Although the models target different tasks as shown in Table 1, they can be easily modified to apply to one another. Currently, as shown in Table 2, the evaluations on this family of methods are still insufficient on the following aspects: (1) some fail to compare with other state-of-the-art models; (2) some are validated only on traffic flow data from taxi or bicycle, not on crowd flow data; (3) some utilize extra data sources such as weather data and POI data; (4) some utilize self-designed objective function; (5) some only utilize RMSE as the evaluation metrics; (6) case studies on some specific regions and times like

¹<https://map.yahoo.co.jp/maps?layer=crowd&v=3>

²<https://lab.its-mo.com/densitymap/>

Table 1. Summary of The State-Of-The-Arts

Model	Reference	Dataset (* means Open)	Prediction Task
ST-ResNet[55]	AAAI17	TaxiBJ*, BikeNYC*	Taxi In-Out Flow (Traffic)
DeepSD[42]	ICDE17	Didi Taxi Request	Taxi Demand (Traffic)
DMVST-Net[48]	AAAI18	Didi Taxi Request	Taxi Demand (Traffic)
Periodic-CRN[62]	IJCAI18	TaxiBJ*, TaxiSG	Taxi Density/In-Out Flow (Traffic)
Hetero-ConvLSTM[53]	KDD18	Vehicle Crash Data*	Traffic Accident (Traffic)
STDN[47]	AAAI19	TaxiNYC*, BikeNYC-II*	Taxi/Bike O-D Number (Traffic)
DeepSTN+[24]	AAAI19	MobileBJ, BikeNYC-I*	Crowd/Taxi In-Out Flow (Crowd&Traffic)
Multitask Model[59]	TKDE19	TaxiBJ, BikeNYC	Taxi/Bike In-Out Flow (Traffic)
DeepUrbanEvent[17]	KDD19	Konzatsu Toukei	Crowd Density/Flow (Crowd)

Table 2. Details of The State-Of-The-Arts

Model	Comparison	Objective Function	Metric	Extra Data
ST-ResNet[55]	[57]	MSE	RMSE	Weather, Event
DeepSD	NA	MSE	MAE, RMSE	Weather, Traffic
DMVST-Net[48]	[55]	Self-Defined	MAPE, RMSE	Weather, Date
Periodic-CRN[62]	[55]	MSE	RMSE	Date
Hetero-ConvLSTM[53]	NA	Cross Entropy (CE)	MSE, RMSE, CE	Weather, Road, etc.
STDN[47]	[42][55][48]	MSE	RMSE, MAPE	Weather, Event
DeepSTN+[24]	[55]	RMSE	RMSE, MAE	Date, PoI
Multitask Model[59]	[57][55]	Self-Defined	RMSE, MAE	Weather, Event
DeepUrbanEvent[17]	[55][7]	MSE	MSE	NA

hot station or residential area in morning rush hour are missing. Thus, in this study, we aim to build a standard benchmark to comprehensively evaluate the state-of-the-art methodologies. Specifically, (1) two classic problems are set as targets: crowd/traffic density prediction and in-out flow prediction [13, 57]. The former is to predict how many people/vehicles will be in each mesh-grid at the next timestamp, and the latter is to predict how many people/vehicles will flow into or out from each mesh-grid in next time interval. The task is to take multiple steps of historical observations as input and report the next-step prediction result as output; (2) A new dataset is created using the GPS log data from a popular smartphone app, which can reflect the real-world crowd density and flow. Then the prediction for crowd and traffic can be conducted by using our new dataset and the existing datasets respectively; (3) Unified objective function MSE is adopted for model training, and extra data source and the related processing module are excluded from the models. So that we can fairly verify the pure ability of video-like modeling on spatiotemporal data; (4) Time-series prediction results on selected regions are added as case studies to demonstrate the effectiveness at different places and times. In summary, our work has three-fold contributions as follows:

- We propose a new concept called video-like urban computing, and give a comprehensive review of the state-of-the-art works of literature.
- We publish a new dataset for crowd density and in-out flow prediction, which is generated based on a real-world smartphone app.
- To the best of our knowledge, this is the first attempt to build a standard benchmark that implements multiple state-of-the-art methods, which are thoroughly evaluated on a set of open datasets.

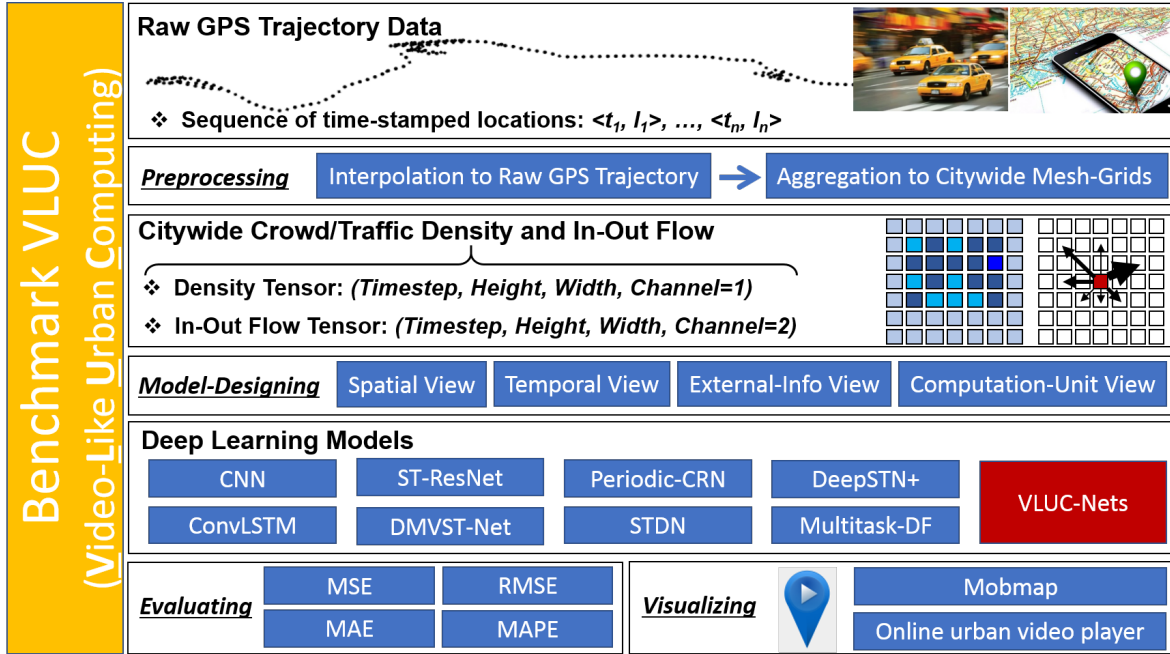


Fig. 2. An overview of benchmark VLUC (Video-Like Urban Computing).

- We develop a family of effective models called VLUC-Nets by empirically integrating the advanced deep learning techniques, and validate its performance and robustness on the benchmark.

An overview of the proposed benchmark VLUC has been shown in Fig.2. With this benchmark, we hope researchers can easily follow up and quickly launch a new solution on this topic.

The remainder of this paper is organized as follows. In Section 2, we introduce data preprocessing and give problem definition. In Section 3, we provide a description of the datasets. In Section 4, we explain the implemented models. In Section 5, we present the evaluation results. In Section 6, we briefly recap some other related works. In Section 7, we give our conclusion and discuss future work.

2 PRELIMINARY

In this section, we first introduce how to do the data preprocessing and then give the problem definition of density and in-out flow prediction. Without loss of generality, in this paper, we use object to refer to people, vehicle, and bicycle in different GPS data sources.

2.1 Data Preprocessing

Object trajectory is represented by a sequence of 3-tuple: $(timestamp, latitude, longitude)$, which be further simplified as a sequence of (t, l) -pair. Object trajectory is stored and indexed by day (i) and object id (o) in the database Γ . Given a time interval $\Delta\tau$, each object's trajectory on each day Γ_{io} is calibrated to obtain constant sampling rate as follows:

$$\Gamma_{io} = (t_1, l_1), \dots, (t_k, l_k), \forall j \in [1, k], |t_{j+1} - t_j| = \Delta\tau$$

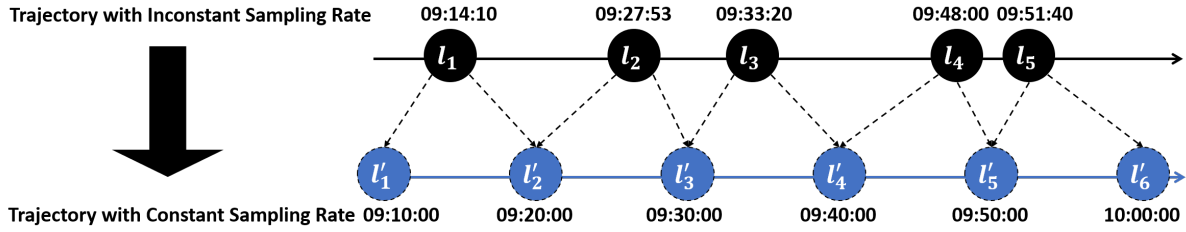


Fig. 3. The illustration of data preprocessing is listed, through which the raw trajectory data with inconstant sampling rate will be calibrated to the trajectories with constant sampling rate. For example, when $\Delta\tau$ is set to 10 minutes, the raw trajectory snippet $\{l_1, l_2, \dots, l_5\}$ timestamped at $\{09:14:10, 09:27:53, \dots, 09:51:40\}$ will be converted to a calibrated trajectory snippet $\{l'_1, l'_2, \dots, l'_6\}$ constantly timestamped at $\{09:10:00, 09:20:00, \dots, 10:00:00\}$. The coordinate value of l'_3 is calculated through linear interpolation based on l_2 and l_3 .

which has been illustrated in Fig.3. Then given the mesh-grids of an urban area $\{g_1, g_2, \dots, g_{Height*Width}\}$, trajectory Γ_{io} is mapped onto mesh-grids as follows:

$$\Gamma_{io} = (t_1, g_1), \dots, (t_k, g_k), \forall j \in [1, k], l_j \in g_j$$

Lastly, density video and in-out flow video can be aggregated and generated with the processed trajectories with constant sampling rate according to the definitions below.

2.2 Problem Definition

Definition 1 (Density and In-Out Flow): Crowd/traffic density at timestamp t in mesh-grid g_m is defined as follows:

$$d_{tm} = |\{o | \Gamma_o.g_t = g_m\}|$$

According to [13, 57], crowd/traffic in-out flow between consecutive timestamps $t-1$ and t in mesh-grid g_m is defined as follows:

$$f_{tm}^{(in)} = |\{o | \Gamma_o.g_{t-1} \neq g_m \wedge \Gamma_o.g_t = g_m\}|$$

$$f_{tm}^{(out)} = |\{o | \Gamma_o.g_{t-1} = g_m \wedge \Gamma_o.g_t \neq g_m\}|$$

Then, by representing the mesh-grids with a 2D index (H, W) , density and in-out flow video containing T consecutive frames can be represented by a 4D tensor $\mathbb{R}^{T \times H \times W \times C}$, where channel C for density and in-out flow are equal to 1 and 2 respectively. Here, Min-Max normalization is used to scale the scalar values into $[0, 1]$.

Definition 2 (Density and In-Out Flow Prediction): Given historical observations of density and in-out flow $x_d = d_1, \dots, d_t, x_f = f_1, \dots, f_t$ at timestamp t , building prediction models for the next-step density and in-out flow $y_d = d_{t+1}, y_f = f_{t+1}$ is to obtain such parameters θ_d, θ_f that can minimize the objective function $\mathcal{L}(\cdot)$ respectively as follows:

$$\theta_d = \underset{\theta_d}{\operatorname{argmin}} \mathcal{L}(\hat{Y}_d, Y_d)$$

$$\theta_f = \underset{\theta_f}{\operatorname{argmin}} \mathcal{L}(\hat{Y}_f, Y_f)$$

where Mean Squared Error (MSE) = $\frac{1}{2} \|Y - \hat{Y}\|^2$ is adopted as $\mathcal{L}(\cdot)$ in our benchmark.

3 DATASET

In this section, we introduce a new dataset and the existing ones used for our benchmark.

Table 3. DataSet Summary

Dataset	Data Type	Mesh Size	H, W	Time Period, Interval	Max Value
BousaiTYO	Density, In-Out Flow	450m×450m	80, 80	2017/4/1/-2017/7/9, 0.5 hour	2965, 887
BousaiOSA	Density, In-Out Flow	450m×450m	60, 60	2017/4/1/-2017/7/9, 0.5 hour	1998, 435
TaxiBJ	In-Out Flow	unknown	32, 32	inconsecutive 4 parts, 0.5 hour	1292
BikeNYC	In-Out Flow	unknown	16, 8	2014/4/1-2014/9/30, 1 hour	267
BikeNYC-I	In-Out Flow	unknown	21, 12	2014/4/1-2014/9/30, 1 hour	737
BikeNYC-II	In-Out Flow	1km×1km	10, 20	2016/7/1-2016/8/29, 0.5 hour	307
TaxiNYC	In-Out Flow	1km×1km	10, 20	2015/1/1-2015/3/1, 0.5 hour	1289

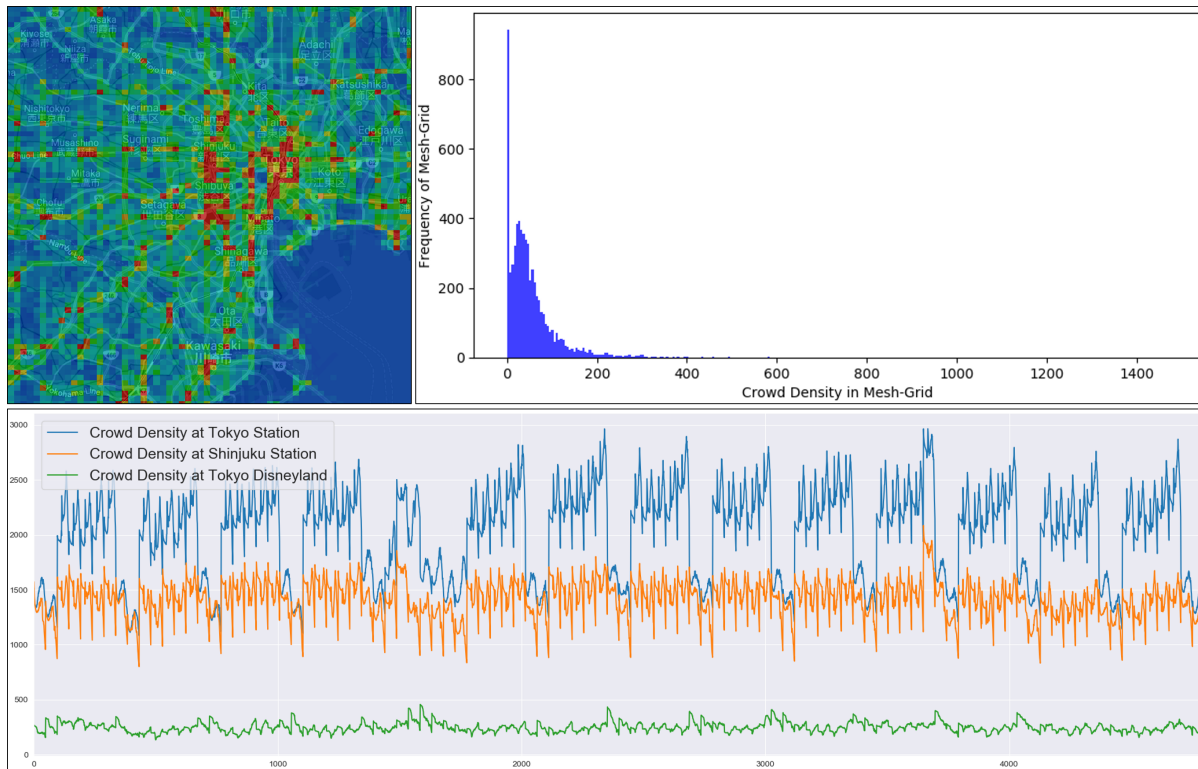


Fig. 4. One snapshot of BousaiTYO density at 2017/4/1 09:00:00 is listed on the upper left, where the red color represents the highest density and the blue color represents the lowest density. The crowd density distribution over the 6,400 mesh-grids is plotted on the upper right. Time-series of crowd density over 100 days (4,800 timestamps) in Tokyo station, Shinjuku station, and Tokyo Disneyland is plotted at the bottom.

3.1 BousaiTYO and BousaiOSA

AAAAA (ANONYMIZED IT COMPANY for blind review) provides a smartphone application called Bousaisokuho to give early information and warning towards different disasters such as earthquake, rain, snow, and tsunami. Users are required to provide their location information so that Bousai App can precisely send local disaster alerts to the users in relevant areas. Also, real-time GPS trajectory data are anonymously collected under users’

consent for real-time notification and research purposes. GPS logs will be generated when the smartphone user stops staying at one location and starts moving by identifying the change of current location. Every day since 2017, the GPS logs are being generated from around 1 million users (approximately 1% of the total population of Japan). The file size of each day is about 18 GB, containing approximately 150 million GPS records. Each record includes user ID, timestamp, latitude, and longitude. The sampling rate of each user's GPS data is approximately 20 records per day, which is similar to common call detail records (CDR) data, but sparser than many taxi GPS data.

We select two big cities in Japan (Tokyo³ and Osaka⁴) as target urban areas, 100 consecutive days from 2017/4/1 to 2017/7/9 as target time period. We crop the raw GPS trajectory data in this spatiotemporal range out. As data preprocessing, we first conduct data cleaning and noise reduction to the raw GPS trajectory data, and then do linear interpolation to make sure each user's 24-hour (00:00~23:59) GPS log has a constant sampling rate with $\Delta\tau$ equal to 5 minutes. To generate video-like data, we mesh each area with $\Delta Lon.=0.005$ $\Delta Lat.=0.004$ (approximately 450m×450m), which results 80×80 and 60×60 mesh-grids respectively for each city. We get one timestamp every 30 minutes, so there are 4800 timestamps (100 days×48/day) in total. According to Definition 1, crowd density and in-out flow are generated for each timestamp. To further eliminate the concerns of user privacy problem, k-anonymization is conducted by setting the scalar values less than 10 to 0. Finally, for Tokyo dataset BousaiTYO, the density and in-out flow video can be represented by tensor (4800, 80, 80, 1) and (4800, 80, 80, 2) respectively; for Osaka dataset BousaiOSA, the density and in-out flow video can be represented by tensor (4800, 60, 60, 1) and (4800, 60, 60, 2) respectively. A series of visualization results about BousaiTYO density data have been listed as Fig.4.

Moreover, in our benchmark, we integrate an online visualization tool called Mobmap (ANONYMIZED URL) to demonstrate the datasets, which can function like a typical video player to play urban video data as shown in Fig.5. By employing the dynamic grid data visualization module of Mobmap, it displays the crowd density variation of Tokyo frame by frame on the map, just like playing a video. The module receives the geographic grid data (timestamp, meshcode, value) as input, outputs the frame-by-frame image data by timestamp aggregation and color mapping. It enables users to observe the trend of grid data over time as if watching a video, which provides a new possibility to find valuable insights. To improve the flexibility of visualization analysis and enhance the observation experience, Mobmap further integrates a series of interactive operations. (1) It provides play, pause, and fast-forward buttons, enabling users to observe on various time scales and specific moments, e.g., Fig.4 shows the crowd density statue at 12:00:00 AM. (2) It provides a set of practical color schemes and allows users to adjust the upper bound of the color mapping based on their requirements (i.e., if the grid value is higher than the bound, it will be mapped to a fixed color). e.g., In Fig.5, we can efficiently define and monitor the hottest regions over time, we chose the No.1 color scheme with the bound set to 100, which means if the grid crowd density is higher than 100, the mapped color will always be red(hottest region). Users can customize color schema and threshold based on data properties, task requirements, and personal preference, to achieve the most reasonable visualization effect.

3.2 TaxiBJ, BikeNYC, and TaxiNYC

TaxiBJ. This is taxi in-out flow data used by [55, 62], created from the taxicab GPS data in Beijing from four separate time periods: 2013/7/1-2013/10/30, 2014/3/1-2014/6/30, 2015/3/1-2015/6/30, and 2015/11/1-2016/4/10.

BikeNYC. This is bike in-out flow data used by [55], taken from the NYC Bike system from 2014/4/1 to 2014/9/30. Similar datasets BikeNYC-I, BikeNYC-II were used by [24] and [47] respectively. These two will be integrated into our benchmark since they have a larger spatial range than BikeNYC.

³Tokyo: *Longitude* ∈ [139.50, 139.90], *Latitude* ∈ [35.50, 35.82]

⁴Osaka: *Longitude* ∈ [135.35, 135.65], *Latitude* ∈ [34.58, 34.82]

0:8 • Renhe Jiang*, Zekun Cai*, Zhaonan Wang, Chuang Yang, Zipei Fan, Xuan Song, Kota Tsubouchi, and Ryosuke Shibasaki

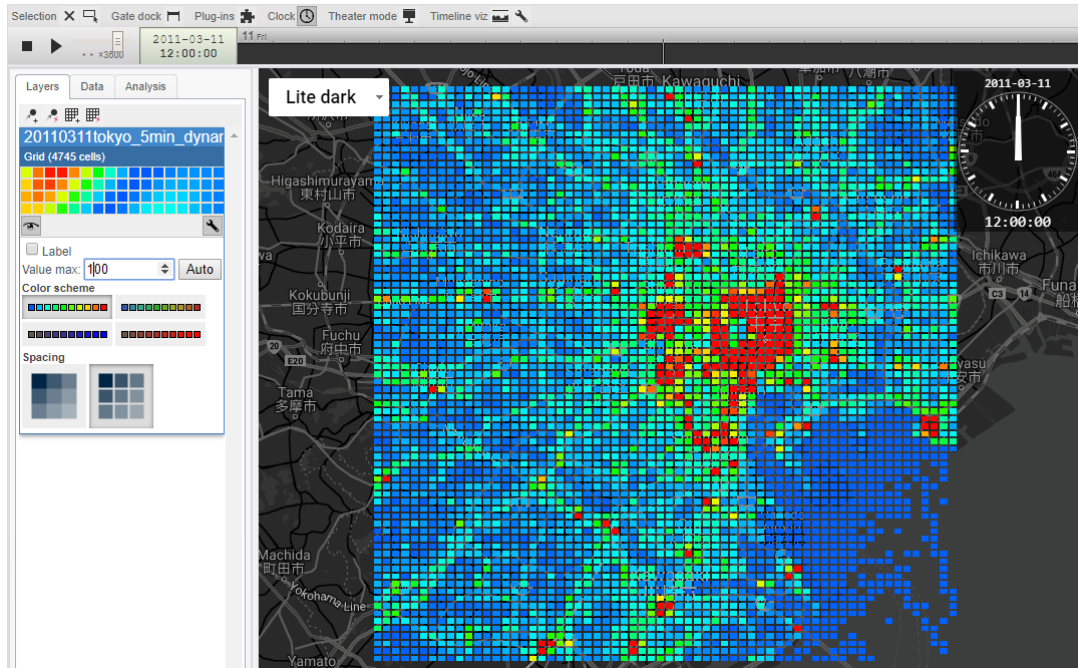


Fig. 5. The online visualization tool (Mobmap) runs like a typical video player for urban video data.

TaxiNYC. This is taxi in-out flow data used by [47], created from the NYC-Taxi data in 2015.

The details of our new dataset, as well as the existing ones, are given in Table 3. Through it, we can see the advantage of our new dataset on the following aspects: (1) large urban area; (2) fine-grained mesh size; (3) high user sampling rate. Our benchmark will integrate BousaiTYO-OSA for crowd density and in-out flow prediction task; TaxiBJ, BikeNYC I-II, and TaxiNYC for traffic in-out flow prediction task.

4 MODEL

In this section, we introduce the models implemented in our benchmark for comparison and evaluation.

4.1 Baselines and The-State-of-The-Arts

HistoricalAverage. Density and in-out flow for each timestamp are estimated by averaging the historical values from the corresponding timestamp in the training dataset, and weekday and weekend will be considered separately.

CopyYesterday. We directly copy the corresponding observation (frame) from the previous day (yesterday) as the result.

CNN. It is a basic deep learning predictor constructed with four CNN layers. The 4D tensor would be converted to 3D tensor ($H, W, T * C$) by concatenating the channels at each timestep just like the way [55] did, so that CNN could take a 4D tensor as input. The CNN predictor utilizes four Conv layers to take the current observed t -step frames as input and predicts the next frame as output. The four Conv layers use a 32 filters of 3×3 kernel window, and the fourth Conv layer uses a ReLU activation function to output the next frame (step) of urban video. BatchNormalization is added between two consecutive layers.

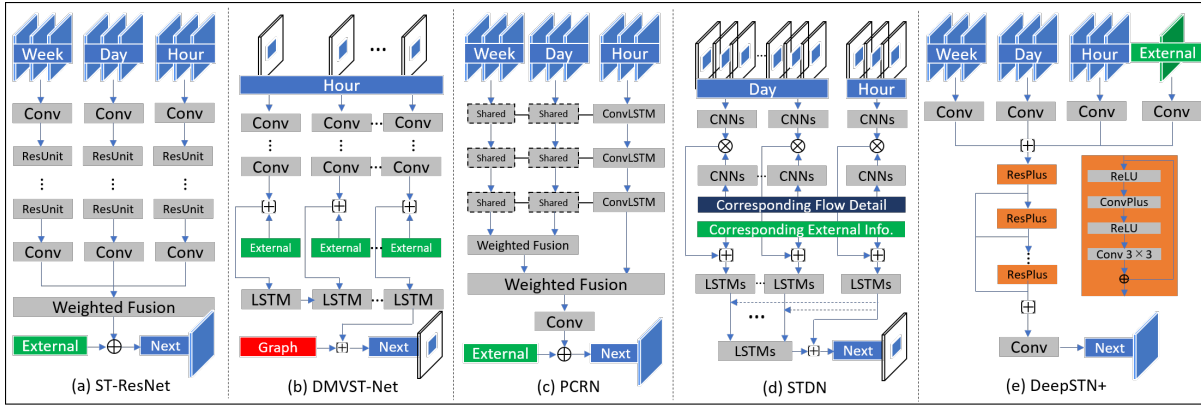


Fig. 6. Model Architecture Summary.

ConvLSTM. Convolutional LSTM [46] extends the fully connected LSTM (FC-LSTM) to have convolutional structures in both the input-to-state and state-to-state transitions. ConvLSTM has achieved new success on video modeling tasks due to its superior performance in capturing both spatial and temporal dependency than CNN. Thus, a stronger predictor can be constructed with four ConvLSTM layers, which also takes current t -step observations as input and predicts the next step. The ConvLSTM layers use a 32 filters of 3×3 kernel window and the ReLU activation is used in the final layer. BatchNormalization is also added between two consecutive layers.

Multitask-DF. Multitask learning [30] was employed by [59] and [17] to model two correlated tasks together and gain concurrent enhancement. Similarly, we design a ConvLSTM-based multitask model to jointly model density and in-out flow video. The motivation comes from the following two points: (1) People tend to follow the trend. Crowded places may attract more and more people to visit; (2) Higher inflow will lead to higher density, higher outflow will lead to lower density. Multitask-DF first takes X_d (t -step observed density) and X_f (t -step observed in-out flow) with two separate ConvLSTM layers; then concatenates two separate latent representations and passes it to two consecutive ConvLSTM layers; finally outputs \hat{Y}_d (next-step density) and \hat{Y}_f (next-step in-out flow) with two separate ConvLSTM layers. The model parameters θ can be trained by minimizing the objective function $\mathcal{L}(\cdot)$ as follows:

$$\theta = \underset{\theta}{\operatorname{argmin}} [\lambda \mathcal{L}(\hat{Y}_d, Y_d) + (1 - \lambda) \mathcal{L}(\hat{Y}_f, Y_f)]$$

where λ is fine-tuned as 0.3 in the experiment. **ConvLSTM** and **Multitask-DF** naturally rely on the superior performance of ConvLSTM to capture both spatial and temporal dependency.

Keeping the same setting with **CNN** and **ConvLSTM**, every ConvLSTM layer uses a 32 filters of 3×3 kernel window, and the ReLU activation is added only in the final layer.

The core architectures of other state-of-the-art models from ST-ResNet to DeepSTN+ are simplified and summarized as Fig.6. They will be comprehensively and uniformly reviewed from the following aspects: (1) core technique to capture spatial and temporal dependency; (2) input feature; (3) computation unit; (4) extra component.

ST-ResNet. ST-ResNet[55] is a CNN-based deep learning method for traffic in-out flow prediction. To capture citywide spatial dependency, it employs residual learning to construct deep enough CNN networks; To capture temporal dependency, it first designs a set of unique features namely *Closeness*, *Period*, and *Trend*, which correspond to *the recent time intervals*, *daily periodicity*, and *weekly trend* respectively, then fuses them together through three learnable parametric matrices. Intuitively, the three sequences can be represented by $[X_{t-l_c},$

$X_{t-(l_c-1)}, \dots, X_{t-1}$], $[X_{t-l_p \cdot p}, X_{t-(l_p-1) \cdot p}, \dots, X_{t-p}]$, and $[X_{t-l_q \cdot q}, X_{t-(l_q-1) \cdot q}, \dots, X_{t-q}]$, where l_c, l_p, l_q are the sequence length of *Closeness*, *Period*, *Trend*, p and q are the span of *Period* and *Trend*, the *Closeness* span is equal to 1 by default. 4D tensor would be converted to 3D tensor (H, W, T^*C) by concatenating the channels at each timestep. The computation unit is the whole citywide image. Additionally, it further utilizes weather, holiday event information, and metadata (i.e. DayOfWeek, Weekday/Weekend) as external information. To verify the pure ability of capturing spatial and temporal dependency, only metadata will be utilized in our benchmark.

DMVST-Net. DMVST-Net[48] is a deep learning method for taxi demand prediction based on CNN and LSTM. It uses a local CNN to capture spatial dependency only among nearby grids; employs LSTM to capture temporal dependency only from the recent time intervals (i.e. *Closeness*). The local CNN takes one grid and its surrounding grids (i.e. $S \times S$ region) as the input, and a separate and unshared CNN is constructed for each timestamp. The input tensor is essentially $(T, S, S, 1)$, and the computation unit is grid (pixel) rather than citywide image. Furthermore, it constructs a weighted graph, where nodes are the grids, and each edge represents the similarity of two time-series values (i.e. historical taxi demand) between any two grids; then it embeds this graph into a feature vector and concatenates it with the main feature vector from LSTM layer. Through this, it can improve the ability to capture citywide spatial dependency. Similarly, in our benchmark, only metadata will be utilized as external information.

PCRN. Periodic-CRN[62] is a ConvGRU-based deep learning model for taxi density and in-out flow prediction by fully making use of recurrent periodic patterns. To capture citywide spatial dependency, it builds a pyramidal architecture by stacking three convolutional RNN layers. To capture temporal dependency, it first learns a representation from the observations of *Closeness* through the stacked pyramidal ConvGRUs; it divides the representations into two types of periodic patterns, namely daily and weekly pattern, each of them is a set of periodic representations corresponding to a specific time span (i.e. day or week); then it maintains a memory-based dictionary to reuse and update the two types of periodic patterns dynamically; lastly it employs a weighting based fusion to merge periodic representations with the current representation of input sequence. Thus, the input feature can be seen as *Closeness*, *Period*, and *Trend*. The computation unit is the whole citywide image. Also, only metadata will be utilized as external information. In our benchmark, we replace ConvGRU with ConvLSTM and simplify the architecture as Fig.6-(c) shows.

STDN. Spatial-Temporal Dynamic Network (STDN)[47] is an improved version of DMVST-Net for taxi/bike Origin-Destination number (volume) prediction. To capture spatial dependency, it inherits the local CNN technique from DMVST-Net, and further designs a flow gating mechanism to fuse local flow information (i.e. flow from one central grid to its surrounding $S \times S$ grids) with the traffic volume information together. In terms of temporal dependency, it improves DMVST-Net by taking not only *Closeness* information but also long-term daily periodicity (i.e. *Period*) into account. Moreover, it considers the temporal shifting problem about periodicity (i.e. traffic data is not strictly periodic) and designs a *Periodically Shifted Attention Mechanism* to solve the issue. Specifically, it sets a small time window to collect Q time intervals right before and after the currently-predicting one. And it uses an LSTM plus attention mechanism to obtain a weighted average representation h from the time intervals in each window. For previous P days to be considered as *Period*, it gets a sequence of representations (h_1, h_2, \dots, h_P) , then it uses another LSTM layer to extract the final periodic representation from the sequence. The computation unit is grid (pixel) same with DMVST-Net. Lastly it jointly models inflow (start traffic volume) and outflow (end traffic volume) together. The flow gating mechanism will be pruned in our benchmark since flow detail information are needed.

DeepSTN+. DeepSTN+ [24] is an improved version of ST-ResNet for crowd and traffic in-out flow prediction. It directly inherits the input features (i.e. *Closeness*, *Period*, and *Trend*), and enhances the ST-ResNet from the following aspects: (1) to capture longer-range spatial dependency, it designs a unique *ConvPlus* block, and replaces the ordinary *Conv*-based residual unit in ST-ResNet with *ResPlus* (i.e. *ConvPlus*-based residual unit). Furthermore, multi-scale fusion mechanism is employed to preserve the representation from each *ResPlus* layer; (2) in terms of temporal dependency, it applies early-fusion mechanism instead of end-fusion in ST-ResNet to get

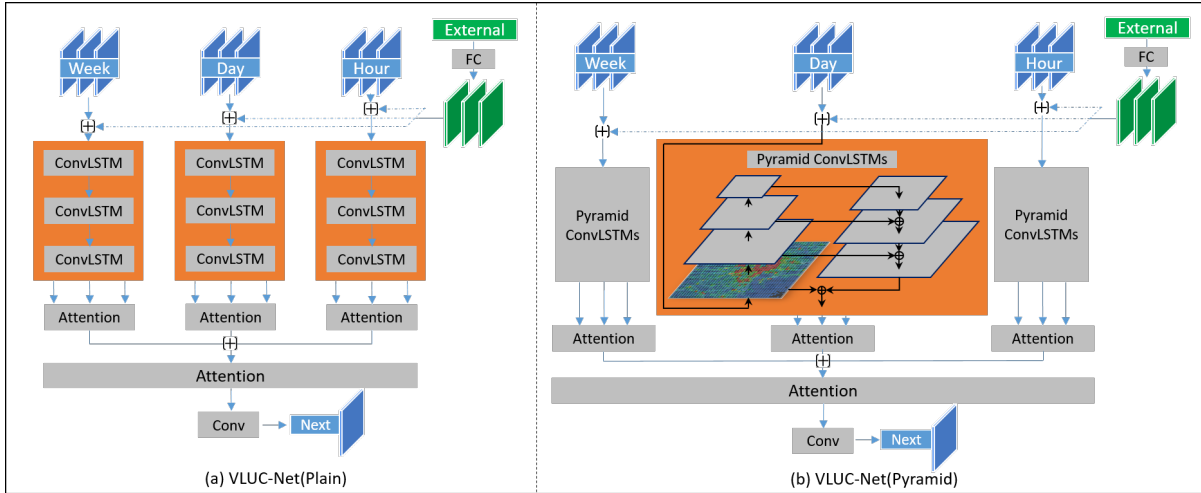


Fig. 7. Architecture of VLUC-Nets: VLUC-Nets with plain ConvLSTMs and VLUC-Nets with pyramid ConvLSTMs.

better interaction among *Closeness*, *Period*, and *Trend*; (3) additionally, it takes the influence of location function on the crowd/traffic flow into consideration by using POI data to gain a semantic plus. The computation unit is the whole citywide image. Similarly, we prune the POI processing component from DeepSTN+ to verify the pure spatiotemporal modeling capability.

4.2 VLUC-Nets

On this benchmark, we propose a novel family of deep learning models named after our benchmark: VLUC-Nets. Through the experience of implementing the state-of-the-arts on the benchmark, we notice that the models with pixel (mesh-grid) as the computing unit will not be so efficient, especially for a large spatial domain like BousaiTYO ($H, W=80, 80$) or BousaiOSA ($H, W=60, 60$). Therefore, we first set the computation unit as the whole citywide image for VLUC-Nets. Moreover, ConvLSTM has demonstrated the advantage on simultaneously capturing the spatial and temporal dependency, thus we build VLUC-Nets by utilizing ConvLSTM as the basic component like the way **PCRN** and **Multitask-DF** did. We inherit and modify the wide used input features *Closeness*, *Period*, and *Trend* as $[X_{(t-T_c)-l_c}, X_{(t-T_c)-(l_c-1)}, \dots, X_{(t-T_c)-1}]$, $[X_{(t-T_p)-l_c}, X_{(t-T_p)-(l_c-1)}, \dots, X_{(t-T_p)-1}]$, and $[X_{(t-T_t)-l_c}, X_{(t-T_t)-(l_c-1)}, \dots, X_{(t-T_t)-1}]$, where T_c , T_p , and T_t represent the periodicity of *Closeness*, *Period*, and *Trend*. On Bousai dataset where the time interval is 30 minutes, when T_c is set to 0, *Closeness* corresponds to the current momentary observations; when T_p is set to 48, *Period* corresponds to the observations from previous day (i.e., daily periodicity); when T_t is set to $7 * 48$, *Trend* corresponds to the observations from previous week (i.e., weekly periodicity). Also, only date information will be utilized as external (meta) information. Finally, after consolidating the basic strategies, VLUC-Nets are elaborately built based on ConvLSTM following the standard model-designing views as shown in Fig.2. Two versions of VLUC-Nets are implemented in our benchmark as shown in Fig.7. The plain version is designed for datasets with small spatial domain, while the pyramid version is designed for datasets with large spatial domain. The concrete techniques are listed as follows:

- **Temporal View.** Attention is all we need[41], and LSTM plus attention mechanism has been seen as a state-of-the-art technique in sequential modeling tasks. Especially, in the urban computing filed, LSTM plus attention has achieved a lot of success on individual's next-location prediction (DeepMove[8]), traffic time prediction for each road path (DeepTTE[43]), and traffic volume and flow prediction (STDN[47]).

Here, we employ and extend the attention mechanism from LSTMs to ConvLSTMs. Originally, for LSTMs, an attention block takes a 3D tensor (*Batch, Timestep, Feature*) as input, and outputs a 2D attention tensor (*Batch, Feature*). Now, for ConvLSTMs, the attention block takes a 5D tensor (*Batch, Timestep, Height, Width, Channel*) as input, and outputs a 4D attention tensor (*Batch, Height, Width, Channel*). The formulas for the attention block are listed as follows:

$$h_{att} = \sum_{i=1}^{l_c} \alpha_i \cdot h_i$$

$$z_i = \tanh(W * h_i + b)$$

$$\alpha_i = \frac{e^{z_i}}{\sum_j e^{z_j}}$$

Here, W is the weights of fully-connected (FC) layers for i -th hidden state in H outputted by ConvLSTM layers. The hidden states of ConvLSTMs $H = \{h_1, h_2, \dots, h_{l_c}\}$ will be fused as one attention state denoted as h_{att} . For each set of ConvLSTMs *Closeness*, *Period*, and *Trend*, each individual attention block will generate an attention state, namely h_{att_c} , h_{att_p} , and h_{att_t} . Then the list of attention states $\{h_{att_c}, h_{att_p}, h_{att_t}\}$ will be further fed into another attention block to fuse the *Closeness*, *Period*, and *Trend* information together as shown in Fig.7-(a).

- **Spatial View.** Extracting and utilizing pyramid and hierarchical features are taken as the state-of-the-art technique in the computer vision-related literatures such as Feature Pyramid Networks (FPN) [22], Mask R-CNN [12], and Faster R-CNN [32]. To better capture the citywide spatial dependency, pyramid ConvLSTMs are utilized to replace the plain-stacked ConvLSTMs as shown in Fig.7-(b), where the outputs from the lower ConvLSTM layers are concatenated with the upper layers. The latent representations derived from pyramid ConvLSTM are considered to contain richer spatial information than the ones from plain ConvLSTMs. In addition, pyramid ConvLSTMs can shorten the distance from the input to output which functions similarly as deep residual networks, but pyramid networks do not require to build a very deep network to gather the upper-level features from the input.
- **External-Info View.** In spatio-temporal city computing applications, external information such as timestamps and other metadata also have significant influences on model performance. Instead of fusing them with fully connected layer or simple convolutional layer, we employed ConvLSTM to explore the complex interactions between spatio-temporal data and metadata. Specifically, external information, including time and day, day of week and holiday flag, are sent to one fully connected layer after one-hot encoding, the output will be reshaped to a 5D tensor (*Batch, Timestep, Height, Width, Channel*) and concatenated with spatio-temporal data to obtain the input of Pyramid ConvLSTMs. This early input mechanism for external enables the model to deeper fuse multiple heterogeneous data and faster convergence.

5 EXPERIMENT

In this section, we present the evaluation results for the state-of-the-art models as well as baseline models.

5.1 Parameter Setting

The following settings were kept the same for each model and dataset. We set the current observation step to 6 (i.e. *Closeness*), and used the corresponding observations from previous 1 day and 1 week as *Period* and *Trend* respectively, which means l_c , T_c , T_p , and T_t are set to $\{6, 0, 7, 7*48\}$ respectively. It should be noted that these settings on *Closeness, Period, Trend* follow the ones widely used and well tuned in the state-of-the-arts listed in Table 1. Data from the first 80% were set as training data (20% of which were taken as validation data), and the

ST-ResNet	DMVST	PCRN	STDN
Residual units: 2 Filters: 32 Kernel size: 3	Neighborhood: 9 Sequence length: 6 Graph embedding: 32 Conv layers: 3 Filters: 32 Kernel size: 3 Spatial output: 64 Temporal output: 512 Semantic output: 6	ConvLSTM layers: 3 Filters: 32 ConvLSTM kernel size: 3 Fusion kernel size: 1 Transform kernel size: W*H	Neighborhood: 9 Short term length: 6 Long term length: 3 Shifted attention: 3 Conv layers: 3 Kernel size: 3 Filters: 32 Hidden output: 128 Drop out: 0.1
Multitask-DF	DeepSTN+	VLUC (Pyramid)	VLUC (Plain)
ConvLSTM layers: 4 Filters: 32 Kernel size: 3	ResPlus units: 2 Channels in ConvPlus: 32 Separated channels: 8 Pooling rate: [8 8 6 6 4 1 1 1] Filters: 32 Kernel size: 1 Drop out: 0.1	ConvLSTM layers: 6 Filters: 32+128, 64+128, 128+128 Kernel size: 3+1, 3+1, 3+1	ConvLSTM layers: 3 Filters: 128 Kernel size: 3

Fig. 8. Summary of fine-tuned hyper-parameters. Note that the parameters displayed in the list [8,8,6,6,4,1,1,1] correspond to the settings for the dataset list [BousaiTYO Density, ..., BikeNYC-I, BikeNYC-II].

other 20% were set as testing data. Adam was employed to control the overall training process, where the batch size was set to 4 and the learning rate was set to 0.0001. The training algorithm would either be early-stopped if the validation error converged within 10 epochs or be stopped after 200 epochs, and the best model on validation data would be saved. We rescaled the predicted value back to the original value. All models were run multiple times on each dataset, and the best result would be recorded. Our benchmark was built based upon Keras[5] and TensorFlow[2]. The experiments were performed on 3 GPU servers, together with six GeForce GTX 1080Ti graphics cards and two Tesla P40 graphics cards. For all approaches, we used grid search to tune the parameters based on the validation dataset and chose the best set of hyperparameters. We also considered the parameter settings recommended by the original study. The hyper-parameters are finely tuned as Fig.8 by spending equal amounts of effort in each.

5.2 Evaluation Metric

We evaluate the effectivenesses of the models with MSE (Mean Squared Error), RMSE (Root Mean Square Error), MAE (Mean Absolute Error), and MAPE (Mean Absolute Percentage Error):

$$MSE = \frac{1}{n} \sum_i^n \|\hat{Y}_i - Y_i\|^2$$

$$RMSE = \sqrt{\frac{1}{n} \sum_i^n \|\hat{Y}_i - Y_i\|^2}$$

$$MAE = \frac{1}{n} \sum_i^n |\hat{Y}_i - Y_i|$$

$$MAPE = \frac{1}{n} \sum_i^n \left| \frac{\hat{Y}_i - Y_i}{Y_i} \right|$$

where n is the number of samples, Y and \hat{Y} are the ground-truth tensor and predicted tensor.

Table 4. Effectiveness Evaluation of Crowd Density and In-Out Flow Prediction on BousaiTYO

Model	Tokyo Density				Tokyo In-Out Flow			
	MSE	RMSE	MAE	MAPE	MSE	RMSE	MAE	MAPE
HistoricalAverage	190.162	13.790	6.866	3.72%	38.183	6.179	1.855	4.15%
CopyYesterday	963.744	31.044	11.531	5.11%	75.911	8.713	2.532	4.65%
CNN	78.642	8.868	3.787	2.19%	42.896	6.550	1.965	4.03%
ConvLSTM	61.363	7.833	3.127	1.85%	14.314	3.783	1.440	3.66%
ST-ResNet	39.900	6.317	3.459	2.05%	11.328	3.366	1.412	3.39%
DMVST-Net	24.194	4.919	2.656	1.59%	21.645	4.652	1.686	3.98%
PCRN	31.192	5.585	3.296	2.14%	17.602	4.195	1.439	3.51%
DeepSTN+	60.937	7.806	3.888	2.91%	10.764	3.281	1.331	3.23%
STDN	23.187	4.815	2.606	1.59%	10.733	3.276	1.472	3.56%
Multitask-DF	38.095	6.172	2.531	1.77%	11.668	3.416	1.406	3.66%
VLUC-Nets (Pyramid)	20.536	4.532	2.432	1.49%	9.760	3.124	1.170	2.97%

Table 5. Effectiveness Evaluation of Crowd Density and In-Out Flow Prediction on BousaiOSA

Model	Osaka Density				Osaka In-Out Flow			
	MSE	RMSE	MAE	MAPE	MSE	RMSE	MAE	MAPE
HistoricalAverage	74.752	8.646	4.826	4.39%	11.510	3.393	0.920	2.73%
CopyYesterday	234.461	15.312	7.375	5.80%	19.417	4.406	1.116	2.89%
CNN	24.017	4.901	2.396	2.20%	50.530	7.108	1.582	3.55%
ConvLSTM	18.646	4.318	2.062	2.03%	6.101	2.470	0.779	2.45%
ST-ResNet	16.522	4.065	2.292	2.09%	4.976	2.231	0.721	2.21%
DMVST-Net	10.571	3.251	1.850	1.77%	8.375	2.894	0.879	2.50%
PCRN	13.549	3.681	2.175	2.22%	6.896	2.626	0.736	2.35%
DeepSTN+	20.762	4.557	2.436	2.80%	5.653	2.378	0.872	2.29%
STDN	11.950	3.457	1.891	1.86%	4.906	2.215	0.801	2.21%
Multitask-DF	13.580	3.685	1.856	1.88%	5.336	2.310	0.731	2.32%
VLUC-Nets (Pyramid)	10.145	3.185	1.760	1.72%	4.887	2.211	0.662	2.18%

5.3 Performance Evaluation

5.3.1 Effectiveness Evaluation. The overall evaluation results on effectiveness are summarized in Table 4~5 for BousaiTYO-OSA, Table 6~7 for TaxiBJ, TaxiNYC, BikeNYC I-II. Through them we can see that the state-of-the-art models including our proposed had advantages compared with baselines (HistoricalAverage~ConvLSTM). In particular, we have the following observations on newly published datasets and the existing ones.

- On bousai dataset, the state-of-the-arts (ST-ResNet~Multitask-DF) had their own advantages on different cities, tasks, and metrics, and none of them could achieve the best results from different points of view.

Table 6. Effectiveness Evaluation of Traffic In-Out Flow Prediction on TaxiBJ and TaxiNYC

Model	TaxiBJ				TaxiNYC			
	MSE	RMSE	MAE	MAPE	MSE	RMSE	MAE	MAPE
HistoricalAverage	2025.328	45.004	24.475	8.04%	463.763	21.535	7.121	4.56%
CopyYesterday	1998.375	44.703	22.454	8.14%	1286.035	35.861	10.164	5.78%
CNN	554.615	23.550	13.797	8.46%	280.262	16.741	6.884	8.08%
ConvLSTM	370.448	19.247	10.816	5.61%	147.447	12.143	4.811	5.16%
ST-ResNet	349.754	18.702	10.493	5.19%	133.479	11.553	4.535	4.32%
DMVST-Net	415.739	20.389	11.832	5.99%	185.601	13.605	4.928	4.49%
PCRN	355.511	18.855	10.926	6.24%	181.091	13.457	5.453	6.27%
DeepSTN+	329.080	18.141	10.126	5.14%	130.407	11.420	4.441	4.45%
STDN	317.764	17.826	9.901	4.81%	126.615	11.252	4.474	4.09%
VLUC-Nets (Plain)	337.754	18.378	10.325	5.40%	113.514	10.654	4.157	4.54%

Table 7. Effectiveness Evaluation of Traffic In-Out Flow Prediction on BikeNYC-I and BikeNYC-II

Model	BikeNYC-I				BikeNYC-II			
	MSE	RMSE	MAE	MAPE	MSE	RMSE	MAE	MAPE
HistoricalAverage	245.743	15.676	4.882	5.45%	23.757	4.874	1.500	3.30%
CopyYesterday	241.681	15.546	4.609	5.36%	54.054	7.352	1.995	3.94%
CNN	145.549	12.064	4.088	5.82%	20.351	4.511	1.574	3.98%
ConvLSTM	43.765	6.616	2.412	3.90%	10.076	3.174	1.133	2.90%
ST-ResNet	37.279	6.106	2.360	3.72%	10.182	3.191	1.169	2.86%
DMVST-Net	63.849	7.990	2.833	3.93%	12.397	3.521	1.287	2.97%
PCRN	130.878	11.440	3.790	4.90%	10.893	3.300	1.185	3.04%
DeepSTN+	38.497	6.205	2.489	3.48%	10.275	3.205	1.245	2.80%
STDN	33.445	5.783	2.410	3.35%	9.022	3.004	1.167	2.67%
VLUC-Nets (Plain)	33.997	5.831	2.175	3.51%	9.725	3.119	1.124	2.89%

The proposed VLUC-Nets with pyramid architecture became the dominant approach, and demonstrate the superiority to the state-of-the-arts as well as VLUC-Nets without pyramid architecture on all of datasets, tasks, and metrics. As the spatial domain (i.e., $H,W=80,80$) of the new published dataset is much larger than the existing datasets, the pyramid architecture plays a vital role in capture the spatial dependency. Next to VLUC-Nets (pyramid-version), STDN also achieved satisfactory performances on all axes. However, as the computation unit of STDN is pixel (mesh-grid), the big spatial domain will generate a huge amount of training samples, so the training process of STDN would take far more time than other models.

- On the existing open datasets, STDN showed the best performances on TaxiBJ, BikeNYC-I, and BikeNYC-II in general, while VLUC-Nets (plain-version) achieved the best performance on TaxiNYC. Since the spatial domain of the existing datasets is relatively small, VLUC-Nets stacked with plain ConvLSTMs demonstrated better performance comparing with pyramid-version VLUC-Nets. Besides, on BikeNYC-I and BikeNYC-II, VLUC-Nets achieved the lowest MAE, and the performances on other three metrics were very close to STDN. On TaxiNYC, STDN could achieve the second best performance. On TaxiBJ, next to STDN, DeepSTN+ ranked at the second place, and VLUC-Nets ranked at the third place. In general,

Table 8. Effectiveness Evaluation of Crowd Density Prediction at Tokyo Station (BousaiTYO Density, RMSE)

Model	Weekday				Weekend			
	08:00	12:00	16:00	20:00	08:00	12:00	16:00	20:00
HistoricalAverage	37.357	117.929	164.000	84.214	13.133	42.267	7.800	22.200
CopyYesterday	23.000	213.000	234.000	127.000	761.000	844.000	998.000	1068.000
CNN	54.531	67.546	38.000	38.261	17.483	21.288	19.923	11.824
ConvLSTM	81.155	115.292	61.783	24.590	26.054	20.643	23.479	11.110
ST-ResNet	38.744	61.021	95.236	66.676	32.790	33.078	33.511	13.608
DMVST-Net	26.504	27.418	37.083	79.421	40.295	26.635	38.955	51.070
PCRN	26.879	21.868	20.620	40.321	14.811	26.793	13.038	1.272
DeepSTN+	101.730	101.602	207.788	184.692	38.459	24.950	26.828	49.394
STDN	43.319	56.437	16.428	10.171	1.900	11.223	7.506	18.041
Multitask-DF	61.564	3.396	27.148	41.094	15.129	0.007	6.681	14.158
VLUC-Nets (Pyramid)	11.217	45.914	0.070	37.548	3.782	8.936	7.699	2.650

Table 9. Effectiveness Evaluation of Crowd Density Prediction at Tokyo Disneyland (BousaiTYO Density, RMSE)

Model	Weekday				Weekend			
	08:00	12:00	16:00	20:00	08:00	12:00	16:00	20:00
HistoricalAverage	46.500	19.000	17.786	26.643	43.133	18.733	6.600	7.667
CopyYesterday	58.000	47.000	42.000	46.000	38.000	23.000	30.000	59.000
CNN	9.447	12.679	5.577	7.747	5.868	0.400	2.330	11.803
ConvLSTM	9.251	9.170	0.462	3.058	6.508	1.895	4.441	12.158
ST-ResNet	13.126	9.128	4.291	12.289	0.890	2.912	0.727	0.102
DMVST-Net	15.761	7.075	1.515	11.274	1.069	2.175	0.631	3.834
PCRN	7.769	5.712	6.085	10.095	4.114	2.080	0.747	11.471
DeepSTN+	25.266	15.173	10.018	11.436	14.299	10.398	12.125	15.217
STDN	18.896	12.237	9.763	4.603	0.445	0.978	0.928	14.851
Multitask-DF	10.727	5.557	12.050	2.570	10.460	10.378	3.371	0.955
VLUC-Nets (Pyramid)	11.443	11.543	8.268	8.278	3.647	1.790	0.065	4.736

on four open datasets, STDN and plain-version VLUC-Nets hold relatively clear advantages over other models. Note that the training process of STDN was still the slowest one on any of the existing datasets.

In contrast to the evaluation from the overall view, we also conducted a very specific evaluation on 1 weekday (last Fri. in BousaiTYO, i.e. 2017/7/7) and 1 weekend (last Sat. in BousaiTYO, i.e. 2017/7/8) in two selected locations (mesh-grids) to show the ground-truth and predicted density. One is the mesh-grid containing Tokyo Station, a typical CBD area, another is the mesh-grid containing Tokyo Disneyland, a popular theme park. RMSE was calculated at four timestamps (08:00, 12:00, 16:00 and 20:00) on each day. From Table 8~9, we can see that the deep learning models had their own advantages at different types of day, times, and locations. In particular, VLUC-Nets had the lowest overall RMSE on BousaiTYO density in Table 4, but it did not overwhelm all the other models at the two case studies in Table 8~9. This demonstrates that the global optimal metric can't assure the local optimal in specific location and time. How to achieve a global-local consistent model will be left as an open challenge and an independent topic that deserves further research effort.

Table 10. Efficiency Evaluation on BousaiTYO Density and In-Out Flow

Model	Tokyo Density			Tokyo In-Out Flow		
	Number of Parameters	Time (s) per Epoch	Epochs to Converge	Number of Parameters	Time (s) per Epoch	Epochs to Converge
CNN	20,929	9	47	22,946	8	22
ConvLSTM	187,432	108	80	189,848	107	94
ST-ResNet	205,095	20	185	297,002	21	121
DMVST-Net	1,578,253	1,669	68	1,578,253	1,684	59
PCRN	1,284,999	300	169	1,561,352	300	167
DeepSTN+	327,820,193	154	38	327,820,546	142	97
STDN	6,181,505	4,895	85	6,349,922	5100	43
Multitask-DF	266,176	150	166	266,176	150	166
VLUC-Nets (Pyramid)	7,882,842	356	107	8,315,355	515	138

Table 11. Efficiency Evaluation on BousaiOSA Density and In-Out Flow

Model	Osaka Density			Osaka In-Out Flow		
	Number of Parameters	Time (s) per Epoch	Epochs to Converge	Number of Parameters	Time (s) per Epoch	Epochs to Converge
CNN	20,929	7	44	22,946	7	16
ConvLSTM	187,432	79	68	189,848	79	119
ST-ResNet	165,895	20	184	218,602	20	120
DMVST-Net	1,578,253	980	50	1,578,253	989	62
PCRN	806,199	170	166	962,152	155	192
DeepSTN+	184,414,913	90	39	184,415,138	90	49
STDN	6,181,505	2,891	85	6,349,922	3,251	55
Multitask-DF	266,176	119	183	266,176	119	183
VLUC-Nets (Pyramid)	6,264,442	267	90	6,512,155	272	66

Table 12. Efficiency Evaluation on TaxiBJ and TaxiNYC

Model	TaxiBJ			TaxiNYC		
	Number of Parameters	Time (s) per Epoch	Epochs to Converge	Number of Parameters	Time (s) per Epoch	Epochs to Converge
CNN	22,946	28	21	22,946	4	67
ConvLSTM	189,848	333	81	189,848	45	74
ST-ResNet	145,984	85	61	123,402	11	75
DMVST-Net	1,578,253	1,222	46	1,578,253	62	83
PCRN	410,398	660	50	234,552	83	80
DeepSTN+	33,607,666	161	33	20,519,858	13	80
STDN	6,349,922	5,950	42	6,349,922	181	34
VLUC-Nets (Plain)	9,567,089	850	32	9,036,923	98	139

Table 13. Efficiency Evaluation on BikeNYC-I and BikeNYC-II

Model	BikeNYC-I			BikeNYC-II		
	Number of Parameters	Time (s) per Epoch	Epochs to Converge	Number of Parameters	Time (s) per Epoch	Epochs to Converge
CNN	22,946	6	57	22,946	4	60
ConvLSTM	189,848	74	95	189,848	47	75
ST-ResNet	124,618	18	54	123,402	11	72
DMVST-Net	1,529,101	107	83	1,578,253	64	68
PCRN	245,440	146	116	234,552	83	85
DeepSTN+	32,554,482	32	62	20,519,858	12	64
STDN	6,349,922	355	45	6,349,922	181	37
VLUC-Nets (Plain)	9,070,171	158	82	9,036,923	104	54

5.3.2 Efficiency Evaluation. Besides the comparison in terms of prediction accuracy, we also provide an efficiency comparison in terms of computational time and neural network complexity between the different approaches, as these can play an important role in practice when deciding which approach to use in practice. Specifically, we study the total number of parameters, training time per epoch in second, and epochs needed to converge for each model on each dataset, which have been listed as Table 10~13. Through the tables, we can see that: (1) the overall efficiency of our proposed VLUC-Nets especially the plain version was controlled at an acceptable level; (2) the training time of DMVST-Net and STDN were far more than others as they took mesh-grid as the computation unit; (3) the parameter number of DeepSTN+ was far more than others as it utilized fully-connected layer to capture the citywide spatial dependency; (4) ST-ResNet holds a very clear advantage over other models from the view of efficiency.

5.3.3 Summary. In summary, the state-of-the-art models designed different techniques to capture spatiotemporal dependency, however, none of them could be acknowledged as a dominant model at the current stage. Their main limitations are as follows: (1) ST-ResNet converts the video-like data to high-dimensional image-like data and uses a simple fusion-mechanism to handle different types of temporal dependency; (2) through the experiment, it was found PCRN took more epochs to converge and tended to cause overfitting; (3) DMVST-Net and STDN use local CNN to take grid (pixel) as computation unit, resulting in long training time (nearly 1 week) on Bousai dataset; (4) DeepSTN+ utilized a fully-connected layer in *ConvPlus* block, which would result in a huge number of parameters in Tokyo area (over 0.3 billion); (5) Multitask-DF needs both density and in-out flow data for computing. Finally, we can do the following recommendations based on the different requests and situations: (1) if effectiveness comes first, pyramid VLUC-Nets will be recommended for datasets with large spatial domain, and STDN will be recommended for small-spatial-domain data; (2) if efficiency comes first, ST-ResNet could be a very light but still powerful solution; (3) if we balance the effectiveness and efficient, plain-version VLUC-Nets could always be a good choice.

6 DISCUSSION

Challenges. Although we try our best to make the benchmark as thorough as possible, there are still some open challenges left to be solved or to be further enhanced.

- **Multi-step predictability.** In our benchmark, crowd/traffic density and in-out flow are defined as a single-step prediction problem. The multi-step predictability could be further validated, and an effective multi-step VLUC-Net is also considered to be proposed.

- Better explainability. Currently, the-state-of-the-arts and the proposed VLUC-Nets still lack of transparent explainability, which has been a major drawback of deep learning-based approaches. As a specific urban computing scenario, we hope to add more explainability to the models using the domain knowledge of geoinformation science.
- Thorough comparison. The current benchmark integrates the most relevant deep learning models following the similar problem definition. However, some trajectory-based prediction models could also be implemented as comparison models such as CityMomentum[7] and DeepMove[8]. Moreover, some pure video prediction models like PredNet[26] proposed and succeeded in the filed of computer vision could also be employed as baseline models.

Applications. This work will be a highly-extendable benchmark, which could be easily applied to other urban computing problems (other than citywide crowd/traffic prediction problems) as listed below. We would like to explore the extendability to these urban computing scenarios in the future.

- Single-channel urban video. Citywide air quality can be represented with an urban tensor ($Timestep, Height, Width, Channel=1$), where $Channel$ stores the PM2.5 value for each mesh-grid. Similarly, citywide electric power consumption could also be represented with that tenor, where $Channel$ stores the aggregated data collected from each electric power meter of the houses inside the mesh-grid.
- Multi-channel urban video. People in city have different transportation behaviors such as by car, train/subway, bike or walk. Citywide transportation demand can be represented by ($Timestep, Height, Width, Channel=4$), where each $Channel$ corresponds to the number of people with one certain transportation mode. Similarly, citywide emergency incidents can also be represented as a multi-channel urban video, where each $Channle$ corresponds to a specific type of incident, such as crime, medical, and fire incidents.
- Super-channel urban video. Inflow and outflow can only indicate how many people will flow into or out from a certain mesh-grid, and can't answer where (which mesh-grid) the people flow come or transit. For a crowd of inside one mesh-grid, their next locations could distributed over the entire mesh $\Omega=(Height,Width)$. Therefor, citywide detailed crowd-flow could be represented with a tensor ($Timestep, Height, Width, Channel=\Omega$), where $Channel$ is super-high dimension.

7 RELATED WORK

In this section, we briefly discuss some existing researches concerning to crowd or traffic prediction problem in the field of urban computing[60]. Except for the video-like deep learning approaches, there are also some statistical models proposed. Spatiality preservable factored Poisson regression [33] incorporates point of interest to overcome data sparsity and degraded performance in even finer grains population prediction. CityProphet[18, 34] and [61] utilize query data of Smartphone App to forecast only crowd density other than crowd flow. [3, 39] conduct transition estimation from aggregated population data, and [40] estimates the transition populations using inflow and outflow defined by [13].

Based on road network, [1, 4, 16, 27–29, 36] were proposed to predict the traffic flow, speed, congestion, human mobility as well as transportation mode. In particular, DeepTTE[45] and DeepGTT[19] are proven as effective deep learning models to predict the travel time on each road segment. Leveraging on the latest techniques, a series of models have been proposed to address traffic-related problems, such as using graph neural networks for traffic forecasting [52] and ride-hailing demand prediction [10], multitask learning for travel time estimation [20], or meta learning for traffic prediction [31].

Besides, many trajectory-based deep learning models were proposed to predict each individual's movement [9, 25, 54]. [25] extends a regular RNN by utilizing time and distance specific transition matrices to propose an ST-RNN model for predicting the next location. DeepMove [8], considered to be a state-of-the-art model for trajectory

prediction, designed a historical attention module to capture periodicities and augment prediction accuracy. VANext[9] further enhanced DeepMove by proposing a novel variational attention mechanism. Modeling human mobility for very large populations [7, 35] and simulating human emergency mobility following disasters [37, 38] are similar problems to ours; however, their models are built based on millions of individuals' mobility. [6] propose tensor factorization approach to decompose urban human mobility, aiming to understand basic urban life patterns from city-scale human mobility data. Using mobility data from location-based social networks (LBSN), [21, 44] design matrix factorization-based models to conduct PoI recommendation or location prediction. Also, [50] utilized latent factor models for POI recommendation using heterogeneous features. [11] conducted chain store site recommendation with transfer learning and multi-source data.

Last, other video-like urban computing problems are also modeled based on citywide mesh-grids, and addressed through advanced deep learning technologies, including air quality prediction[23, 49], crop yield prediction[51], crime prediction[15], and abnormal event prediction[14].

8 CONCLUSION AND FUTURE WORK

In this study, we build a standard benchmark called VLUC for video-like computing on citywide traffic and crowd prediction by publishing new datasets called BousaiTYO and BousaiOSA and integrating the existing ones including TaxiBJ, BikeNYC I-II, and TaxiNYC. An online visualization tool called Mobmap can function like a typical video player on those data. We comprehensively and systematically review the state-of-the-art works of literature including ST-ResNet, DMVST-Net, PCRN, STDN, DeepSTN+, and Multitask-DF, and conduct a thorough performance evaluation for those models on density and in-out flow prediction problems. We empirically design a family of models named as VLUC-Nets by employing the advanced deep learning techniques to more effectively capture spatial and temporal dependency. The experimental results demonstrate the superior performances of VLUC-Nets to the state-of-the-arts on both new datasets and the existing ones. This benchmark <https://github.com/deepkashiwa20/VLUC> will be officially published including the new dataset if this paper is accepted.

In the future, apart from the used metrics like RMSE, MAE, and MAPE, some supplemental metrics are considered to be introduced, such as Hausdorff Distance, Longest Common Subsequence (LCSS), and Dynamic Time Warping (DTW) to verify the time-series similarity, or KL-Divergence and Cross Entropy to verify probability distribution. Then, the effects of different settings on the use of heterogeneous data sources such as POI and event info, objective function, and scaling strategy could be further analyzed. Moreover, we will continue to explore the limitations of the state-of-the-arts as well as our proposed models, and try to improve the performances on the benchmark. Lastly, as discussed above, we will try to address the open challenges and apply this family of approaches to other video-like urban computing problems, such as citywide air quality prediction, and citywide crime incident prediction.

ACKNOWLEDGMENTS

REFERENCES

- [1] Afshin Abadi, Tooraj Rajabioun, and Petros A Ioannou. 2014. Traffic flow prediction for road transportation networks with limited traffic data. *IEEE transactions on intelligent transportation systems* 16, 2 (2014), 653–662.
- [2] Martín Abadi, Ashish Agarwal, Paul Barham, Eugene Brevdo, Zhifeng Chen, Craig Citro, Greg S. Corrado, Andy Davis, Jeffrey Dean, Matthieu Devin, Sanjay Ghemawat, Ian Goodfellow, Andrew Harp, Geoffrey Irving, Michael Isard, Yangqing Jia, Rafal Jozefowicz, Lukasz Kaiser, Manjunath Kudlur, Josh Levenberg, Dan Mané, Rajat Monga, Sherry Moore, Derek Murray, Chris Olah, Mike Schuster, Jonathon Shlens, Benoit Steiner, Ilya Sutskever, Kunal Talwar, Paul Tucker, Vincent Vanhoucke, Vijay Vasudevan, Fernanda Viégas, Oriol Vinyals, Pete Warden, Martin Wattenberg, Martin Wicke, Yuan Yu, and Xiaoqiang Zheng. 2015. TensorFlow: Large-Scale Machine Learning on Heterogeneous Systems. <http://tensorflow.org/> Software available from tensorflow.org.
- [3] Yasunori Akagi, Takuya Nishimura, Takeshi Kurashima, and Hiroyuki Toda. 2018. A Fast and Accurate Method for Estimating People Flow from Spatiotemporal Population Data.. In *IJCAI*. 3293–3300.

- [4] Pablo Samuel Castro, Daqing Zhang, and Shijian Li. 2012. Urban traffic modelling and prediction using large scale taxi GPS traces. In *Pervasive Computing*. Springer, 57{72.
- [5] Francois Chollet. 2015. keras. <https://github.com/fchollet/keras>.
- [6] Zipei Fan, Xuan Song, and Ryosuke Shibasaki. 2014. CitySpectrum: a non-negative tensor factorization approach. *Proceedings of the 2014 ACM International Joint Conference on Pervasive and Ubiquitous Computing*, 13{223.
- [7] Zipei Fan, Xuan Song, Ryosuke Shibasaki, and Ryutaro Adachi. 2015. CityMomentum: an online approach for crowd behavior prediction at a citywide level. In *Proceedings of the 2015 ACM International Joint Conference on Pervasive and Ubiquitous Computing*, 559{569.
- [8] Jie Feng, Yong Li, Chao Zhang, Funing Sun, Fanchao Meng, Ang Guo, and Depeng Jin. 2018. Deepmove: Predicting human mobility with a sequential recurrent networks. In *Proceedings of the 2018 World Wide Web Conference*. International World Wide Web Conferences Steering Committee, 1459{1468.
- [9] Qiang Gao, Fan Zhou, Goce Trajcevski, Kunpeng Zhang, Ting Zhong, and Fengli Zhang. 2019. Predicting human mobility via variational attention. In *The World Wide Web Conference*. ACM, 2750{2756.
- [10] Xu Geng, Yaguang Li, Leye Wang, Lingyu Zhang, Qiang Yang, Jieping Ye, and Yan Liu. 2019. Spatiotemporal multi-graph convolution network for ride-hailing demand forecasting. In *2019 AAAI Conference on Artificial Intelligence (AAAI)*, 19.
- [11] Bin Guo, Jing Li, Vincent W Zheng, Zhu Wang, and Zhiwen Yu. 2018. Citytransfer: Transferring inter-and intra-city knowledge for chain store site recommendation based on multi-source urban data. *Proceedings of the ACM on Interactive, Mobile, Wearable and Ubiquitous Technologies*, 4 (2018), 135.
- [12] Kaiming He, Georgia Gkioxari, Piotr Dollar, and Ross Girshick. 2017. Mask R-CNN. In *IEEE International Conference on Computer Vision (ICCV)*.
- [13] Minh X Hoang, Yu Zheng, and Ambuj K Singh. 2016. Forecasting citywide crowd flows based on big data. *SIGSPATIAL* (2016).
- [14] Chao Huang, Chuxu Zhang, Jiashu Zhao, Xian Wu, Nitesh Chawla, and Dawei Yin. 2019. MiST: A Multiview and Multimodal Spatial-Temporal Learning Framework for Citywide Abnormal Event Forecasting. In *The World Wide Web Conference*. ACM, 717{728.
- [15] Chao Huang, Junbo Zhang, Yu Zheng, and Nitesh V Chawla. 2018. DeepCrime: a sensitive hierarchical recurrent networks for crime prediction. In *Proceedings of the 27th ACM International Conference on Information and Knowledge Management*, 1423{1432.
- [16] Wenhao Huang, Guojie Song, Haikun Hong, and Kunqing Xie. 2014. Deep architecture for traffic flow prediction: Deep belief networks with multitask learning. *Intelligent Transportation Systems, IEEE Transactions on*, 15, 5 (2014), 2191{2201.
- [17] Renhe Jiang, Xuan Song, Dou Huang, Xiaoya Song, Tianqi Xia, Zekun Cai, Zhaonan Wang, Kyoung-Sook Kim, and Ryosuke Shibasaki. 2019. DeepUrbanEvent: A System for Predicting Citywide Crowd Dynamics at Big Events. *Proceedings of the 25th ACM SIGKDD International Conference on Knowledge Discovery & Data Mining*, 2114{2122.
- [18] Tatsuya Konishi, Mikiya Maruyama, Kota Tsubouchi, and Masamichi Shimosaka. 2016. CityProphet: city-scale irregularity prediction using transit app logs. In *Proceedings of the 2016 ACM International Joint Conference on Pervasive and Ubiquitous Computing*, 752{757.
- [19] Xiucheng Li, Gao Cong, Aixin Sun, and Yun Cheng. 2019. Learning Travel Time Distributions with Deep Generative Model. In *World Wide Web Conference*. ACM, 1017{1027.
- [20] Yaguang Li, Kun Fu, Zheng Wang, Cyrus Shahabi, Jieping Ye, and Yan Liu. 2018. Multi-task representation learning for travel time estimation. In *Proceedings of the 24th ACM SIGKDD International Conference on Knowledge Discovery & Data Mining*, 1704.
- [21] Defu Lian, Cong Zhao, Xing Xie, Guangzhong Sun, Enhong Chen, and Yong Rui. 2014. GeoMF: joint geographical modeling and matrix factorization for point-of-interest recommendation. In *Proceedings of the 20th ACM SIGKDD international conference on Knowledge discovery and data mining*. ACM, 831{840.
- [22] Tsung-Yi Lin, Piotr Dollar, Ross Girshick, Kaiming He, Bharath Hariharan, and Serge Belongie. 2017. Feature Pyramid Networks for Object Detection. In *The IEEE Conference on Computer Vision and Pattern Recognition (CVPR)*.
- [23] Yijun Lin, Nikhit Mago, Yu Gao, Yaguang Li, Yao-Yi Chiang, Cyrus Shahabi, and Luis Ambite. 2018. Exploiting spatiotemporal patterns for accurate air quality forecasting using deep learning. *Proceedings of the 26th ACM SIGSPATIAL International Conference on Advances in Geographic Information Systems*. ACM, 359{368.
- [24] Ziqian Lin, Jie Feng, Ziyang Lu, Yong Li, and Depeng Jin. 2019. DeepSTN+: Context-aware Spatial-Temporal Neural Network for Crowd Flow Prediction in Metropolis. *AAAI*.
- [25] Qiang Liu, Shu Wu, Liang Wang, and Tieniu Tan. 2016. Predicting the next location: A recurrent model with spatial and temporal contexts. In *Thirtieth AAAI Conference on Artificial Intelligence*.
- [26] William LoŠer, Gabriel Kreiman, and David Cox. 2016. Deep predictive coding networks for video prediction and unsupervised learning. *arXiv preprint arXiv:1605.08120* (2016).
- [27] Yisheng Lv, Yanjie Duan, Wenwen Kang, Zhengxi Li, and Fei-Yue Wang. 2015. Traffic flow prediction with big data: a deep learning approach. *Intelligent Transportation Systems, IEEE Transactions on*, 16, 5 (2015), 865{873.
- [28] Xiaolei Ma, Zhimin Tao, Yin Hai Wang, Haiyang Yu, and Yunpeng Wang. 2015. Long short-term memory neural network for traffic speed prediction using remote microwave sensor data. *Transportation Research Part C: Emerging Technologies*, 54 (2015), 187{197.

- [29] Xiaolei Ma, Haiyang Yu, Yunpeng Wang, and Yinhai Wang. 2015. Large-scale transportation network congestion evolution prediction using deep learning theory. *PLoS one* 10, 3 (2015), e0119044.
- [30] Jiquan Ngiam, Aditya Khosla, Mingyu Kim, Juhan Nam, Honglak Lee, and Andrew Y Ng. 2011. Multimodal deep learning. In *Proceedings of the 28th international conference on machine learning (ICML-11)*. 689–696.
- [31] Zheyi Pan, Yuxuan Liang, Weifeng Wang, Yong Yu, Yu Zheng, and Junbo Zhang. 2019. Urban Traffic Prediction from Spatio-Temporal Data Using Deep Meta Learning. In *Proceedings of the 25th ACM SIGKDD International Conference on Knowledge Discovery & Data Mining*. ACM, 1720–1730.
- [32] Shaoqing Ren, Kaiming He, Ross Girshick, and Jian Sun. 2015. Faster R-CNN: Towards Real-Time Object Detection with Region Proposal Networks. In *Advances in Neural Information Processing Systems 28*, C. Cortes, N. D. Lawrence, D. D. Lee, M. Sugiyama, and R. Garnett (Eds.). Curran Associates, Inc., 91–99. <http://papers.nips.cc/paper/5638-faster-r-cnn-towards-real-time-object-detection-with-region-proposal-networks.pdf>
- [33] Masamichi Shimosaka, Yuta Hayakawa, and Kota Tsubouchi. 2019. Spatiality Preservable Factored Poisson Regression for Large-Scale Fine-Grained GPS-Based Population Analysis. In *Proceedings of the AAAI Conference on Artificial Intelligence*, Vol. 33. 1142–1149.
- [34] Masamichi Shimosaka, Keisuke Maeda, Takeshi Tsukiji, and Kota Tsubouchi. 2015. Forecasting urban dynamics with mobility logs by bilinear Poisson regression. In *Proceedings of the 2015 ACM international joint conference on pervasive and ubiquitous computing*. ACM, 535–546.
- [35] Chaoming Song, Tal Koren, Pu Wang, and Albert-László Barabási. 2010. Modelling the scaling properties of human mobility. *Nature Physics* 6, 10 (2010), 818–823.
- [36] Xuan Song, Hiroshi Kanasugi, and Ryosuke Shibasaki. 2016. DeepTransport: Prediction and Simulation of Human Mobility and Transportation Mode at a Citywide Level. In *IJCAI*. 2618–2624.
- [37] Xuan Song, Quanshi Zhang, Yoshihide Sekimoto, Teerayut Horanont, Satoshi Ueyama, and Ryosuke Shibasaki. 2013. Modeling and probabilistic reasoning of population evacuation during large-scale disaster. In *Proceedings of the 19th ACM SIGKDD international conference on Knowledge discovery and data mining*. ACM, 1231–1239.
- [38] Xuan Song, Quanshi Zhang, Yoshihide Sekimoto, Ryosuke Shibasaki, Nicholas Jing Yuan, and Xing Xie. 2015. A Simulator of Human Emergency Mobility following Disasters: Knowledge Transfer from Big Disaster Data. In *Twenty-Ninth AAAI Conference on Artificial Intelligence*.
- [39] Akihito Sudo, Takehiro Kashiyama, Takahiro Yabe, Hiroshi Kanasugi, Xuan Song, Tomoyuki Higuchi, Shinfiya Nakano, Masaya Saito, and Yoshihide Sekimoto. 2016. Particle filter for real-time human mobility prediction following unprecedented disaster. In *Proceedings of the 24th ACM SIGSPATIAL International Conference on Advances in Geographic Information Systems*. ACM, 5.
- [40] Yusuke Tanaka, Tomoharu Iwata, Takeshi Kurashima, Hiroyuki Toda, and Naonori Ueda. 2018. Estimating Latent People Flow without Tracking Individuals. In *IJCAI*. 3556–3563.
- [41] Ashish Vaswani, Noam Shazeer, Niki Parmar, Jakob Uszkoreit, Llion Jones, Aidan N Gomez, Lukasz Kaiser, and Illia Polosukhin. 2017. Attention is all you need. In *Advances in neural information processing systems*. 5998–6008.
- [42] Dong Wang, Wei Cao, Jian Li, and Jieping Ye. 2017. DeepSD: supply-demand prediction for online car-hailing services using deep neural networks. In *2017 IEEE 33rd International Conference on Data Engineering (ICDE)*. IEEE, 243–254.
- [43] Dong Wang, Junbo Zhang, Wei Cao, Jian Li, and Yu Zheng. 2018. When will you arrive? estimating travel time based on deep neural networks. In *Thirty-Second AAAI Conference on Artificial Intelligence*.
- [44] Yingzi Wang, Nicholas Jing Yuan, Defu Lian, Linli Xu, Xing Xie, Enhong Chen, and Yong Rui. 2015. Regularity and conformity: Location prediction using heterogeneous mobility data. In *Proceedings of the 21th ACM SIGKDD International Conference on Knowledge Discovery and Data Mining*. ACM, 1275–1284.
- [45] Zheng Wang, Kun Fu, and Jieping Ye. 2018. Learning to estimate the travel time. In *Proceedings of the 24th ACM SIGKDD International Conference on Knowledge Discovery & Data Mining*. ACM, 858–866.
- [46] SHI Xingjian, Zhou rong Chen, Hao Wang, Dit-Yan Yeung, Wai-Kin Wong, and Wang-chun Woo. 2015. Convolutional LSTM network: A machine learning approach for precipitation nowcasting. In *Advances in neural information processing systems*. 802–810.
- [47] Huaxiu Yao, Xianfeng Tang, Hua Wei, Guanjie Zheng, and Zhenhui Li. 2019. Revisiting spatial-temporal similarity: A deep learning framework for traffic prediction. In *AAAI Conference on Artificial Intelligence*.
- [48] Huaxiu Yao, Fei Wu, Jintao Ke, Xianfeng Tang, Yitian Jia, Siyu Lu, Pinghua Gong, Jieping Ye, and Zhenhui Li. 2018. Deep multi-view spatial-temporal network for taxi demand prediction. In *Thirty-Second AAAI Conference on Artificial Intelligence*.
- [49] Xiuwen Yi, Junbo Zhang, Zhaoyuan Wang, Tianrui Li, and Yu Zheng. 2018. Deep distributed fusion network for air quality prediction. In *Proceedings of the 24th ACM SIGKDD International Conference on Knowledge Discovery & Data Mining*. ACM, 965–973.
- [50] Hongzhi Yin, Weiqing Wang, Hao Wang, Ling Chen, and Xiaofang Zhou. 2017. Spatial-aware hierarchical collaborative deep learning for POI recommendation. *IEEE Transactions on Knowledge and Data Engineering* 29, 11 (2017), 2537–2551.
- [51] Jiaxuan You, Xiaocheng Li, Melvin Low, David Lobell, and Stefano Ermon. 2017. Deep Gaussian process for crop yield prediction based on remote sensing data. In *Thirty-First AAAI Conference on Artificial Intelligence*.

- [52] Bing Yu, Haoteng Yin, and Zhanxing Zhu. 2018. Spatio-temporal graph convolutional networks: a deep learning framework for traffic forecasting. In *Proceedings of the 27th International Joint Conference on Artificial Intelligence*. AAAI Press, 3634–3640.
- [53] Zhuoning Yuan, Xun Zhou, and Tianbao Yang. 2018. Hetero-ConvLSTM: A Deep Learning Approach to Traffic Accident Prediction on Heterogeneous Spatio-Temporal Data. In *Proceedings of the 24th ACM SIGKDD International Conference on Knowledge Discovery & Data Mining*. ACM, 984–992.
- [54] Chao Zhang, Keyang Zhang, Quan Yuan, Luming Zhang, Tim Hanratty, and Jiawei Han. 2016. Gmove: Group-level mobility modeling using geo-tagged social media. In *Proceedings of the 22nd ACM SIGKDD International Conference on Knowledge Discovery and Data Mining*. ACM, 1305–1314.
- [55] Junbo Zhang, Yu Zheng, and Dekang Qi. 2017. Deep Spatio-Temporal Residual Networks for Citywide Crowd Flows Prediction.. In *AAAI*. 1655–1661.
- [56] Junbo Zhang, Yu Zheng, Dekang Qi, and Ruiyuan Li. 2016. Xiuwen Yi. Dnn-based prediction model for spatio-temporal data. In *Proceedings of the 24th ACM SIGSPATIAL International Conference on Advances in Geographic Information Systems*, Vol. 92.
- [57] Junbo Zhang, Yu Zheng, Dekang Qi, Ruiyuan Li, and Xiuwen Yi. 2016. DNN-based prediction model for spatio-temporal data. In *Proceedings of the 24th ACM SIGSPATIAL International Conference on Advances in Geographic Information Systems*. ACM, 92.
- [58] Junbo Zhang, Yu Zheng, Dekang Qi, Ruiyuan Li, Xiuwen Yi, and Tianrui Li. 2018. Predicting citywide crowd flows using deep spatio-temporal residual networks. *Artificial Intelligence* 259 (2018), 147–166.
- [59] Junbo Zhang, Yu Zheng, Junkai Sun, and Dekang Qi. 2019. Flow Prediction in Spatio-Temporal Networks Based on Multitask Deep Learning. *IEEE Transactions on Knowledge and Data Engineering* (2019).
- [60] Yu Zheng, Licia Capra, Ouri Wolfson, and Hai Yang. 2014. Urban computing: concepts, methodologies, and applications. *ACM Transactions on Intelligent Systems and Technology (TIST)* 5, 3 (2014), 38.
- [61] Jingbo Zhou, Hongbin Pei, and Haishan Wu. 2018. Early Warning of Human Crowds Based on Query Data from Baidu Maps: Analysis Based on Shanghai Stampede. In *Big Data Support of Urban Planning and Management*. Springer, 19–41.
- [62] Ali Zonoozi, Jung-jae Kim, Xiao-Li Li, and Gao Cong. 2018. Periodic-CRN: A Convolutional Recurrent Model for Crowd Density Prediction with Recurring Periodic Patterns.. In *IJCAI*. 3732–3738.

Received November 2019